AJSM PreView, published on August 4, 2014 as doi:10.1177/0363546514541225

Winner of the 2014 Excellence in Research Award

Posterior Cruciate Ligament Graft Fixation Angles, Part 1

Biomechanical Evaluation for Anatomic Single-Bundle Reconstruction

Nicholas I. Kennedy,* BS, Robert F. LaPrade,*† MD, PhD, Mary T. Goldsmith,* MSc, Scott C. Faucett,* MD, MSc, Matthew T. Rasmussen,* BS, Garrett A. Coatney,* BS, Lars Engebretsen,‡ MD, PhD, and Coen A. Wijdicks,*§ PhD
Investigation performed at the Department of BioMedical Engineering of the Steadman Philippon Research Institute, Vail, Colorado, USA

Background: Currently, no consensus exists for the optimal graft fixation angle for anatomic single-bundle (SB) posterior cruciate ligament reconstructions (PCLRs). Additionally, direct graft forces have not been measured. Alternative graft fixation angles and the resultant graft forces should be investigated to optimize the stability of SB PCLRs without overconstraining the knee.

Hypothesis: Graft fixation angles of 75°, 90°, and 105° for SB PCLR were hypothesized to improve knee stability compared with the sectioned posterior cruciate ligament state with no evidence of knee overconstraint.

Study Design: Controlled laboratory study.

Methods: Nine fresh-frozen human cadaveric knees were biomechanically evaluated for the intact, sectioned, and SB PCLR states with the anterolateral bundle graft fixed at 75°, 90°, and 105°. A 6 degrees of freedom robotic system assessed knee laxity with a 134-N posterior load applied at 0° to 120° and 5-N·m external, 5-N·m internal, and 10-N·m valgus rotation torques applied at 60° to 120°. By securing the graft to an external load cell, graft forces were measured throughout kinematic testing.

Results: No significant kinematic differences were found among the 3 fixation angles. Each fixation angle resulted in significantly less posterior translation than in the sectioned state at all flexion angles ($P < .05$), with 4.1 mm of average residual laxity during an applied posterior loading. For all graft fixation angles, internal rotation was significantly increased between 60° and 120° of flexion, and external rotation was significantly increased at 90°, 105°, and 120° of flexion compared with the intact state. Graft forces were not significantly different among the 3 fixation angles and remained below reported loads observed during activities of daily living.

Conclusion: All tested SB PCLR graft fixation angles restored knee laxity to similar levels; however, persistent laxity resulted in significant increases in knee laxity compared with the intact state during posterior tibial loading at all flexion angles, internal rotation at flexion angles $\geq$60°, and external rotation at $\geq$75° of flexion.

Clinical Relevance: The results of this study suggest that SB PCL graft fixation angles of 75°, 90°, and 105° were comparable in restoring knee kinematics and exposed the graft to similar time-zero loads. However, SB PCLRs did not fully reduce knee laxity to the intact state.

Keywords: posterior cruciate ligament (PCL); single-bundle PCL reconstruction; graft fixation angles; knee kinematics; graft forces; anterolateral bundle (ALB)

The posterior cruciate ligament (PCL) is the largest intra-articular ligament in the tibiofemoral joint. It is composed of 2 functional bundles, the anterolateral bundle (ALB) and the posteromedial bundle, with each demonstrating the ability to resist posterior tibial translation throughout a full range of knee motion.[1,13,29] The larger ALB reportedly tensions in knee flexion, while the smaller posteromedial bundle has been reported to become taut during extension.[10,22,24,35] Functionally, the PCL is a primary restraint to posterior tibial translation at all flexion angles and internal rotation beyond 90° and a supplemental restraint to external tibial rotation beyond 90° of flexion.[10,15,17,19]

Single-bundle (SB) PCL reconstruction (PCLR) remains the most clinically implemented intraoperative PCLR technique.[6,21] Reconstruction typically consists of an SB PCLR graft primarily aiming to restore the function of the

The American Journal of Sports Medicine, Vol. XX, No. X
DOI: 10.1177/0363546514541225

ALB.[3,6,38] Although advances in SB PCLR objective biomechanical outcomes have been achieved through investigation into optimal tunnel placement and type of fixation,[8,13,14,25,31,33,38] there has been limited research regarding optimal graft fixation angles.[14] Identification of the optimal angle for graft fixation is essential to PCLR success. Less-than-optimal graft fixation angles can potentially introduce either overconstraint, which may limit the joint's range of motion and predispose the graft to premature failure, or underconstraint, which may lead to residual laxity. With clinical and biomechanical reports suggesting that residual laxity remains after SB PCLR,[9,20,37,38] optimization of SB PCLR graft fixation angle may confer additional reductions in laxity and consequently lead to improved objective clinical outcomes for SB PCLR.

A previous biomechanical study evaluated the effect of fixation angles on SB PCLR performance.[14] Harner et al[14] examined 0°, 60°, and 90° as potential graft fixation angles and reported significant differences among the angles in kinematics and cadaveric in situ forces. In addition, other studies have suggested that PCL graft fixation at 90° might provide the best opportunity of restoring knee kinematics to the intact state, especially at increased flexion angles.[26,30] Yet the selection of the 90° fixation angle was stated as a limitation in prior work,[25] because this single tested fixation angle was based on a limited quantity of biomechanical research. However, in a recent study, Kennedy et al[19] evaluated an increased flexion range (0°-120°) for testing and reported that complete sectioning of the PCL resulted in the largest increase in posterior translation at 105°. To our knowledge, no studies have reported on the effects of varying SB PCLR graft fixation angles on knee kinematics and graft forces throughout the range of 0° to 120°. Moreover, there are limited biomechanical data characterizing the effect that graft fixation angle has for flexion angles beyond 90° or when comparing clinically reported fixation angles between 75° and 105°.[5,7,16,32,36] As a result, biomechanical analysis is needed to validate this range of SB PCLR graft fixation angles to validate future clinical use.

Currently, there exists no consensus on the optimal angles for graft fixation during SB PCLR. Therefore, the purpose of this study was to assess graft force and kinematic differences between clinically relevant SB PCLR graft fixation angles compared with the intact and sectioned PCL states. It was hypothesized that all graft fixation angles would significantly reduce laxity compared with the sectioned state and prevent graft overload but that fixation at 105° would result in the greatest reduction in laxity and the best approximation of the intact PCL state. It was anticipated that this information would provide biomechanical data to support the use of different graft fixation angles in SB PCLR.

MATERIALS AND METHODS

Specimen Preparation

Nine fresh-frozen human cadaveric knees (mean age, 52.3 years; range, 29-63 years; mean body mass index, 23.0 kg/m^2; 6 male, 3 female; 4 right, 5 left) were used in this study. The contralateral knees of each specimen were used in part 2 of this study,[18] investigating double-bundle PCLR graft fixation angles. The right and left knees of each pair were randomized between parts 1 and 2 of this study. Only knees without evidence of prior injury, surgery, or abnormality were included in this study. Specimens were stored at –20°C and thawed 24 hours before use. All soft tissue was removed 10 cm from the joint line on both the femur and tibia. The proximal end of the femur and distal end of the tibia were potted in poly(methyl methacrylate) (Fricke Dental) to mount them in the testing apparatus.

Robotic Setup

Intact, reconstructed, and sectioned PCL state biomechanics were collected using a previously described 6 degrees of freedom robotic system (KUKA KR 60-3; KUKA Robotics).[11,19,38,39] The knees were mounted in an inverted orientation with the potted tibia and fibula attached to a custom fixture mounted to a universal force-torque sensor (Delta F/T Transducer; ATI Industrial Automation) at the robotic end effector (Figure 1). A coordinate system was defined for each knee using a coordinate measuring device (MicroScribe MX; GoMeasure3D) to select palpable anatomic landmarks while the knee was neutrally aligned and in full extension.[12,40]

The passive flexion-extension path of each knee from 0° (or full extension) to 120° was determined in 1° flexion increments using robotic position and force control. A 10-N axial load was applied to ensure proper contact between the tibial plateau and femoral condyles while forces and torques at each flexion angle in the remaining 5 degrees of freedom were minimized (<5 N and <0.5 N·m, respectively). The knee positions determined from collecting the passive path were used as the starting points for laxity measurement for each testing condition.

§Address correspondence to Coen A. Wijdicks, PhD, Department of BioMedical Engineering, Steadman Philippon Research Institute, 181 W Meadow Drive, Suite 1000, Vail, CO 81657, USA (e-mail: cwijdicks@sprivail.org).

*Steadman Philippon Research Institute, Vail, Colorado, USA.

†The Steadman Clinic, Vail, Colorado, USA.

‡Department of Orthopaedic Surgery, Oslo University Hospital and Faculty of Medicine, University of Oslo, Oslo, Norway.

Presented at the 40th annual meeting of the AOSSM, Seattle, Washington, July 2014.

One or more of the authors has declared the following potential conflict of interest or source of funding: R.F.L. and L.E. are paid consultants for Arthrex Inc and receive research support from Smith & Nephew. This research was supported by Norwegian Health South-East (Helse Sor-Ost) Regional Health Authority Post-Doctoral Grant No. 39385. Arthrex Inc and Smith & Nephew donated surgical supplies, and AlloSource donated allograft ligament specimens.

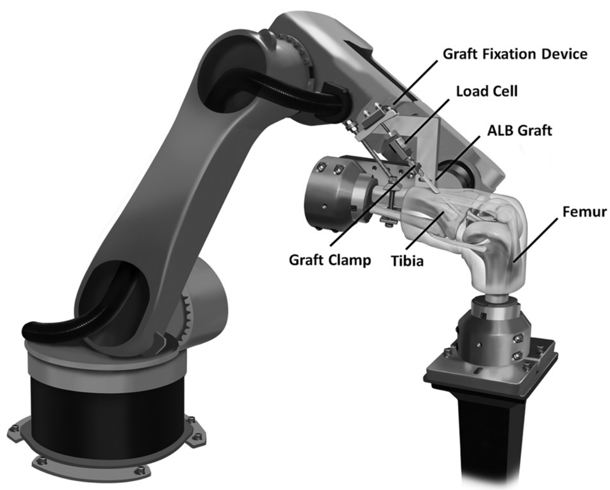

Figure 1. A left knee is shown mounted within the robotic system in an inverted orientation. The femur is fixed to a stationary pedestal, and the tibia and fibula are attached to a universal force-torque sensor affixed to the end effector of a KUKA KR 60-3 robotic system. A single-bundle posterior cruciate ligament reconstruction is shown, with the graft fixed to an external load cell for concurrent acquisition of graft force measurements. ALB, anterolateral bundle.

Graft Preparation

Achilles tendon allografts (AlloSource) were used to reconstruct the ALB of the PCL for the SB PCLR. Grafts were prepared in a similar fashion to previously reported biomechanical and clinical studies.[34,38] The tendinous end was trimmed and tubularized using braided polyblend No. 5 suture (FiberWire; Arthrex) to 11 mm in diameter from the calcaneal bone block to a point on the tendon 150 mm proximal using a graft sizing block. The calcaneal bone plug was prepared to be 11 mm in diameter and 25 mm in length. The calcaneal bone plug was also prepared with 2 passing sutures placed through the plug.

SB PCLR Technique

A single orthopaedic surgeon (S.F.C.) performed all surgical procedures while the knee remained mounted in the robot in an inverted orientation. The SB PCLR technique has been previously described[38] and is similar to a previously reported clinical technique.[34] In brief, the knee was first positioned at 0° of flexion, and a posteromedial incision was used to visualize and identify the tibial footprint of both bundles of the PCL. Both bundles were then carefully transected at the tibial footprint to preserve the integrity of the ligament of Wrisberg (when present). The tibial bundle ridge, an osseous landmark that has been reported to identify the center of the PCL attachment, was then identified.[2] An eyelet pin was drilled through the bundle ridge in a manner that allowed it to exit the anterior tibia 1 cm medial to the tibial tuberosity and 6 cm distal to the joint line. A transtibial tunnel was then drilled using an 11-mm acorn-tipped reamer (Arthrex).

Next, the knee was positioned at 90° of flexion. The PCL femoral footprint was visualized through an anterolateral parapatellar arthrotomy, and both bundles were transected at the femoral attachments. The ALB femoral footprint was used as an anatomic landmark for creating the ALB graft's femoral tunnel. An 11-mm acorn-tipped reamer was centered over the ALB femoral footprint and used as a guide for inserting the eyelet pin. After insertion of the eyelet pin, the acorn-tipped reamer was used to ream a closed socket, 11 mm–diameter femoral tunnel to a depth of 25 mm. With the eyelet pin positioned in the femoral tunnel, the passing suture attached to the calcaneal bone plug was then passed through the eyelet, and this pin was used to pull the sutures through the tunnel. This then allowed the calcaneal bone plug to be pulled into the closed socket tunnel and secured in the femoral tunnel with a 7 × 25–mm titanium screw (Cannulated Interference Screw; Arthrex). A tunnel smoother (9.5-mm Gore Smoother; Smith & Nephew) was passed from anterior to posterior through the tibial tunnel to remove any bony debris and to smooth the proximal aperture of the tibial tunnel. The smoother was used to deliver the passing sutures of the Achilles graft distally through the tibial tunnel. The graft was then secured in the custom graft fixation device, as outlined below. The arthrotomy was closed separately, and the anterior and posterior incisions were sutured closed.

Custom Graft Fixation Device and Graft Force Data Acquisition

To determine the tension on the ALB graft throughout biomechanical testing, the soft tissue end of the graft that exited the tibia was inserted into a custom graft clamp that was attached to a load cell (model 60050-100; Vishay Intertechnology) rigidly mounted to a custom graft fixation device attached to the end effector of the robot. The load cell was calibrated to within 0.25% accuracy using a calibrated tensile testing machine (ElectroPuls E10000; Instron) before biomechanical testing. The graft fixation device allowed unlimited positional adjustability of the load cell and graft to ensure axial alignment with the distal tibial tunnel exit. Once the load cell was aligned, the graft fixation device was locked in place to provide rigid fixation relative to the robotic end effector.

Before distal graft fixation within the custom graft clamp, the graft was manually tensioned to 250 N a total of 10 times to ensure proper passage of the graft through the tibial tunnel, minimize creep effects, and eliminate the potential for initial graft slippage.[27] Next, the knee was robotically cycled through the full range of flexion angles 5 times before distal graft fixation to the load cell. For final graft fixation, the distal graft end was secured in the graft clamp within 3 cm of exiting the tunnel, and the graft was tensioned to 88 N while a 134-N anterior tibial load was robotically applied to the knee to reduce posterior subluxation of the tibia.[14] Load data for each graft were acquired during testing with a data acquisition

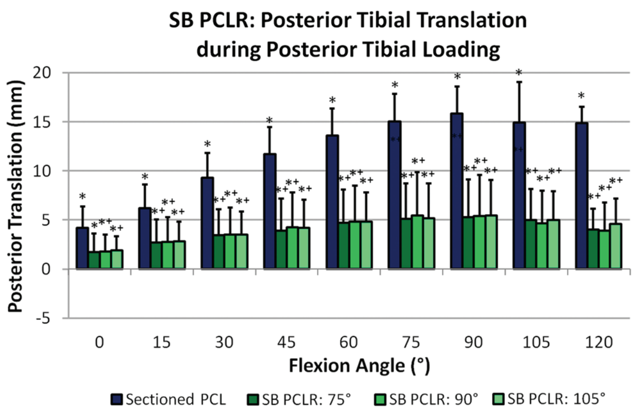

Figure 2. Changes in posterior translation under an applied 134-N tibial load after complete sectioning of the posterior cruciate ligament (PCL) and single-bundle (SB) PCL reconstruction (PCLR) with varying graft fixation angles. Data are reported as average increases of posterior translation compared with the intact PCL knee, with SD bars included. *Significantly different from intact. $^{+}$Significantly different from the sectioned PCL state ($P < .05$).

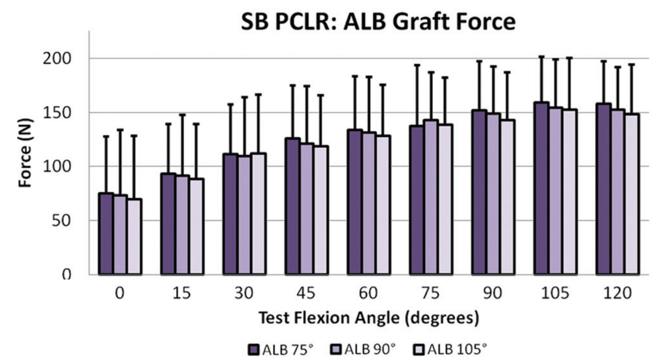

Figure 3. Single-bundle (SB) graft forces measured during an applied 134-N posterior tibial load. Data are reported as mean graft force with SD bars. ALB, anterolateral bundle; PCLR, posterior cruciate ligament reconstruction.

conditioner (Model D4; Micro-Measurements). Loads were recorded at maximum displacement for each test condition after the applied tibio-femoral loads were achieved.

Biomechanical Testing

Intact, reconstructed, and sectioned PCL knees were subjected to a 134-N posterior tibial load[1,13,19,23,28,38] at 0°, 15°, 30°, 45°, 60°, 75°, 90°, 105°, and 120° of flexion, and 5-N·m external, 5-N·m internal, and 10-N·m valgus rotational torques were applied at 60°, 75°, 90°, 105°, and 120° of flexion. The selected flexion angles were based on previously published data demonstrating that significant laxity resulted throughout the range of flexion for the sectioned PCL during applied loads at these particular flexion angles.[19,38] SB PCLR graft fixation angles of 75°, 90° and 105° were investigated for each specimen, and the order of fixation angle testing was randomized for all specimens. Between the testing of each graft fixation angle, the graft was loosened and retensioned to the aforementioned loads before fixation at the new angle. The orders of flexion angles for biomechanical laxity testing during reconstruction were randomized to limit incremental testing bias. After the testing of the intact and reconstructed states, the PCL sectioned state was tested after the removal of all grafts and hardware.

Statistical Analysis

Student *t* tests were used to analyzed differences in kinematics between intact, reconstructed, and sectioned states after each applied loading condition (posterior tibial load, external rotation, internal rotation, and valgus rotation). One-sample *t* tests were used to compare the sectioned and SB PCLR groups individually with the intact state. Two-sample *t* tests were used for comparison between the SB PCLR groups and the PCL sectioned state. Paired-samples *t* tests were used to compare the 3 fixation angles with one another. A 2-factor mixed model analysis was used to examine the relationships of both fixation angles and tested flexion angles and their ability to predict the desired outcome measure of graft force. All statistical analysis was performed using SPSS version 20 (IBM). Within the *t* test comparisons, the Levene test was used to check for equality of variance, and the Welch *t* test was used when groups had significantly different variances. Bonferroni corrections were performed individually within each flexion angle for both the intact and sectioned comparisons and the comparisons among the reconstructed fixation angle states. For all comparisons, significance was declared for Bonferroni-corrected *P* values $< .05$.

RESULTS

Biomechanical Response to Posterior Tibial Load

When subjected to a 134-N posterior tibial load, the PCL sectioned state had significantly more posterior tibial translation compared with the intact state at all flexion angles ($P < .001$) (Figure 2). No significant differences in posterior tibial translation were found among the 3 graft fixation angles for the SB PCLRs. All 3 fixation angles had significantly less posterior translation (Table 1) compared with the sectioned state but significantly more than the intact state at all tested angles of flexion ($P < .05$), except for fixation at 75°, which was not significantly different from intact ($P = .052$) at 0° of flexion. At 90° of flexion, at which the posterior drawer test is performed clinically, there was an increase in posterior translation of 15.8 ± 2.8 mm ($P < .001$) for the PCL sectioned state compared with the intact state. The 75°, 90°, and 105° graft fixation angles had residual increases in translation of 5.3 ± 3.8 mm ($P = .006$), 5.4 ± 4.2 mm ($P = .009$), and 5.4 ± 3.6 mm ($P = .004$), respectively, compared with the intact state at 90° of flexion.

During an applied posterior tibial load, no significant differences were observed between graft forces for any of

TABLE 1
SB Posterior Tibial Translation and Graft Forces During an Applied 134-N Posterior Tibial Load[a]

	Posterior Translation, mm	Change in Posterior Translation From Intact, mm				Graft Forces, N		
			SB PCLR			SB PCLR		
Flexion Angle, deg	Intact (n = 9)	Sectioned (n = 9)	Fixed at 75° (n = 9)	Fixed at 90° (n = 9)	Fixed at 105° (n = 9)	Fixed at 75° (n = 9)	Fixed at 90° (n = 9)	Fixed at 105° (n = 9)
0	8.1 ± 1.7	4.2 ± 2.2[b]	1.7 ± 1.9[b]	1.8 ± 1.7[b,c]	1.9 ± 1.4[b,c]	75 ± 52	73 ± 60	70 ± 59
15	9.0 ± 1.3	6.2 ± 2.4[b]	2.7 ± 2.3[b,c]	2.7 ± 2.6[b,c]	2.8 ± 2.0[b,c]	93 ± 46	91 ± 56	88 ± 51
30	8.7 ± 1.6	9.3 ± 2.5[b]	3.5 ± 2.6[b,c]	3.5 ± 2.8[b,c]	3.5 ± 2.4[b,c]	112 ± 46	110 ± 55	112 ± 54
45	7.2 ± 1.8	11.7 ± 2.7[b]	3.9 ± 3.3[b,c]	4.3 ± 3.5[b,c]	4.2 ± 2.9[b,c]	126 ± 49	121 ± 53	119 ± 48
60	6.0 ± 1.7	13.6 ± 2.7[b]	4.7 ± 3.4[b,c]	4.8 ± 3.6[b,c]	4.8 ± 3.0[b,c]	134 ± 50	131 ± 52	128 ± 47
75	5.2 ± 1.0	15.1 ± 2.8[b]	5.1 ± 3.7[b,c]	5.4 ± 4.5[b,c]	5.2 ± 3.6[b,c]	138 ± 56	143 ± 44	139 ± 43
90	5.5 ± 1.2	15.8 ± 2.8[b]	5.3 ± 3.8[b,c]	5.4 ± 4.2[b,c]	5.4 ± 3.6[b,c]	152 ± 45	149 ± 44	143 ± 44
105	6.3 ± 1.5	14.9 ± 4.2[b]	5.0 ± 3.1[b,c]	4.6 ± 3.3[b,c]	5.0 ± 2.9[b,c]	159 ± 43	155 ± 45	153 ± 47
120	7.4 ± 1.6	14.9 ± 1.6[b]	4.0 ± 2.1[b,c]	3.9 ± 2.9[b,c]	4.6 ± 2.6[b,c]	158 ± 39	152 ± 39	148 ± 46

[a]Data are expressed as mean ± SD. PCLR, posterior cruciate ligament reconstruction; SB, single-bundle.
[b]Significant difference ($P < .05$) from intact state.
[c]Significant difference ($P < .05$) from posterior cruciate ligament sectioned state.

the 3 fixation angles (Figure 3). Maximum graft forces for all 3 graft fixation angles were observed at 105° of flexion during an applied posterior tibial load; maximum graft forces for fixation angles of 75°, 90°, and 105° were 159 ± 43, 155 ± 45, and 153 ± 47 N, respectively. Fixation angle was not a significant contributor to SB PCL graft force ($P = .256$), but instead, the tested flexion angle was a significant contributor to SB PCL graft force ($P < .001$) when pooled across the 3 tested fixation angles. The positive linear relationship between the tested flexion angle and graft force revealed that for every 1° increase in tested flexion angle, there was an approximately 0.67-N increase in graft force.

Biomechanical Response to Internal Rotation Torque

Under an applied 5-N·m internal rotation torque, the PCL sectioned state resulted in significantly more internal rotation at all flexion angles compared with the intact state ($P < .02$). There were no significant differences in internal rotation among the 3 graft fixation angles (Table 2). Each of the 3 graft fixation angle groups had significantly more internal rotation than did the intact state at all flexion angles but significantly less than the sectioned state at 75°, 90°, 105°, and 120° of flexion ($P < .05$). The 75°, 90°, and 105° fixation angles resulted in significant increases in rotation of 1.8° ± 1.2° ($P < .01$), 1.9° ± 1.3° ($P < .01$), and 1.9° ± 1.2° ($P < .01$), respectively, compared with the intact state at 90° of flexion.

Graft forces measured during an applied internal rotation torque demonstrated no significant differences between graft fixation angles. Maximum graft forces were observed at 120° of flexion for fixation at 75° with a graft force of 94 ± 27 N; at 105° and 120° of flexion for fixation at 90° with graft forces of 90 ± 39 and 90 ± 25 N, respectively; and at 105° of flexion for fixation at 105° with a graft force of 85 ± 38 N.

Biomechanical Response to External Rotation Torque

When subjected to a 5-N·m external rotation torque, the PCL sectioned state had significantly more external rotation compared with the intact state for all tested flexion angles greater than 60° of flexion ($P < .05$; $P = .145$ for 60° of flexion). No significant differences existed among the 3 graft fixation angles (Table 2). All 3 fixation angles had significantly more external rotation than did the intact state at flexion angles >75° ($P < .05$), but none were significantly different from the sectioned state. Compared with the intact state, the 75°, 90°, and 105° fixation angles had significant increases in rotation of 1.9° ± 1.8° ($P < .03$), 2.0° ± 1.8° ($P < .03$), and 1.8° ± 1.6° ($P < .02$), respectively, at 90° of flexion.

Graft forces measured during an applied external rotation torque demonstrated no significant differences among graft fixation angles. The magnitude of the measured graft force increased as flexion angle increased for all 3 fixation angles. The maximum graft forces were observed at 120° of flexion, at which the observed forces were 115 ± 44, 109 ± 34, and 99 ± 37 N for fixation angles of 75°, 90°, and 105°, respectively. Notably, measured graft forces at 120° of flexion were approximately double the observed forces at 60° of flexion.

Biomechanical Response to Valgus Rotation Torque

After PCL sectioning, there were significant increases in valgus rotation at 60°, 75°, and 90° of flexion ($P < .05$). No significant differences in valgus rotation existed among the 3 graft fixation angles (Table 3). Each of the 3 graft fixation angles had significantly less valgus rotation than did the sectioned state at 90° of flexion ($P < .05$). No differences existed between the fixation angles and the intact state.

Graft forces measured during an applied valgus rotation torque demonstrated no significant differences among

TABLE 2
SB Tibial Rotation and Graft Forces During Applied 5-N·m Internal and External Torques

Internal Rotation								
	Internal Rotation, deg	Change in Internal Rotation From Intact, deg				Graft Forces, N		
			SB PCLR			SB PCLR		
Flexion Angle, deg	Intact (n = 9)	Sectioned (n = 9)	Fixed at 75° (n = 9)	Fixed at 90° (n = 9)	Fixed at 105° (n = 9)	Fixed at 75° (n = 9)	Fixed at 90° (n = 9)	Fixed at 105° (n = 9)
60	19.2 ± 10.2	2.6 ± 2.1[b]	1.5 ± 1.3[b]	1.5 ± 1.6[b]	1.4 ± 1.5[b]	55 ± 36	53 ± 40	47 ± 35
75	18.2 ± 9.3	3.2 ± 1.5[b]	1.6 ± 1.0[b,c]	1.6 ± 1.1[b,c]	1.4 ± 0.8[b,c]	77 ± 35	73 ± 41	66 ± 37
90	17.9 ± 9.1	4.3 ± 1.7[b]	1.8 ± 1.2[b,c]	1.9 ± 1.3[b,c]	1.9 ± 1.2[b,c]	82 ± 33	80 ± 39	68 ± 39
105	18.0 ± 9.1	4.7 ± 1.5[b]	2.4 ± 1.5[b,c]	2.3 ± 1.6[b,c]	2.3 ± 1.4[b,c]	93 ± 32	90 ± 39	85 ± 38
120	18.9 ± 9.2	4.7 ± 2.0[b]	2.4 ± 1.5[b,c]	2.4 ± 1.7[b,c]	2.3 ± 1.5[b,c]	94 ± 27	90 ± 25	83 ± 33

External Rotation								
	External Rotation, deg	Change in External Rotation From Intact, deg				Graft Forces, N		
			SB PCLR			SB PCLR		
Flexion Angle, deg	Intact (n = 9)	Sectioned (n = 9)	Fixed at 75° (n = 9)	Fixed at 90° (n = 9)	Fixed at 105° (n = 9)	Fixed at 75° (n = 9)	Fixed at 90° (n = 9)	Fixed at 105° (n = 9)
60	18.8 ± 10.8	4.5 ± 6.6	3.8 ± 6.6	3.8 ± 6.8	3.7 ± 6.7	55 ± 38	55 ± 48	48 ± 45
75	20.7 ± 8.7	2.6 ± 2.4[b]	1.9 ± 2.1	2.0 ± 2.3	1.8 ± 1.6[b]	78 ± 36	74 ± 48	66 ± 49
90	21.5 ± 8.3	2.4 ± 2.2[b]	1.9 ± 1.8[b]	2.0 ± 1.8[b]	1.8 ± 1.6[b]	91 ± 43	89 ± 46	79 ± 51
105	22.0 ± 8.1	2.7 ± 1.8[b]	1.9 ± 1.3[b]	2.0 ± 1.3[b]	1.8 ± 1.2[b]	107 ± 39	106 ± 39	92 ± 51
120	21.8 ± 7.8	2.3 ± 1.9[b]	1.3 ± 1.3[b]	1.4 ± 1.1[b]	1.3 ± 1.4[b]	115 ± 44	109 ± 34	99 ± 37

[a]Data are expressed as mean ± SD. PCLR, posterior cruciate ligament reconstruction; SB, single-bundle.
[b]Significant difference ($P < .05$) from intact state.
[c]Significant difference ($P < .05$) from posterior cruciate ligament sectioned state.

TABLE 3
SB Tibial Rotation and Graft Forces During an Applied 10-N·m Valgus Torque

	Valgus Rotation, deg	Change in Valgus Rotation From Intact, deg				Graft Forces, N		
			SB PCLR			SB PCLR		
Flexion Angle, deg	Intact (n = 9)	Sectioned (n = 9)	Fixed at 75° (n = 9)	Fixed at 90° (n = 9)	Fixed at 105° (n = 9)	Fixed at 75° (n = 9)	Fixed at 90° (n = 9)	Fixed at 105° (n = 9)
60	4.7 ± 2.4	1.1 ± 1.0[b]	0.5 ± 1.0	0.5 ± 1.0	0.4 ± 0.9	43 ± 21	43 ± 27	38 ± 25
75	4.4 ± 2.1	1.3 ± 1.1[b]	0.2 ± 0.5[c]	0.4 ± 0.7	0.3 ± 0.6	57 ± 27	55 ± 28	49 ± 30
90	4.7 ± 2.2	1.5 ± 1.2[b]	0.1 ± 0.6[c]	0.1 ± 0.5[c]	0.2 ± 0.5[c]	62 ± 25	61 ± 28	53 ± 32
105	6.0 ± 3.2	0.3 ± 2.0	–0.4 ± 1.8	–0.4 ± 1.6	–0.2 ± 1.5	77 ± 30	76 ± 31	66 ± 35
120	7.0 ± 3.8	0.8 ± 2.0	–0.6 ± 2.4	–0.5 ± 2.1	0.2 ± 0.7	94 ± 52	85 ± 41	72 ± 35

[a]Data are expressed as mean ± SD. PCLR, posterior cruciate ligament reconstruction; SB, single-bundle.
[b]Significant difference ($P < .05$) from intact state.
[c]Significant difference ($P < .05$) from posterior cruciate ligament sectioned state.

fixation angles. For flexion angles >60°, graft forces for graft fixation at 75° were consistently greater than forces for graft fixation at 90°, which were greater than forces for graft fixation at 105°, although these differences were not significant. The magnitude of the measured graft force increased as flexion angle increased for all 3 fixation angles, and the maximum graft forces were observed at 120° of flexion, at which the observed forces were 94 ± 52, 85 ± 41, and 72 ± 35 N for fixation angles of 75°, 90°, and 105°, respectively.

DISCUSSION

The results of this study demonstrated that SB PCLR graft fixation angles of 75° to 105° significantly reduced posterior tibial translation compared with the PCL sectioned state without overconstraining the knee or causing significant changes in graft loading throughout the full range of tested flexion angles. Additionally, there were no significant kinematic differences among the 3 different SB PCL graft fixation angles for posterior translation, internal rotation, external rotation, or valgus rotation. Although the SB PCLR graft fixation angles were effective in significantly reducing the sectioned state's posterior translation and internal rotation, significant increases in posterior translation, internal rotation, and external rotation compared with the intact state demonstrated residual laxity despite investigation into an optimized graft fixation angle. This observation is in agreement with reported biomechanical and clinical laxity remaining after SB PCLR.[4,20,37,38]

Kinematic similarities among the tested graft fixation angles in this study may be explained through anatomic PCL bundle motion and interaction analyses. Ahmad et al[1] and Papannagari et al[29] both reported that the native ALB remains nearly constant in length between 90° and 120° of flexion. In the present study, the measured graft forces and translations during an applied posterior tibial load were similar between 75° and 120° of flexion for all fixation angles. Constant ALB length throughout this range of motion may impart similar kinematics and result in similar transmission of forces through the graft for all graft fixation angles in this range.

Similar to the kinematic response, the forces within the SB PCLR graft during the simulated clinical examinations did not vary significantly across the 3 fixation angles. Although there were no significant differences in the amount of graft load, we believe that there may potentially be some clinical relevance to the higher measured loads that resulted from the 75° fixation angle. Thus, in light of there being no difference in the joint kinematics among the 3 tested graft fixation angles, we recommend future studies examine whether preferentially fixing SB PCLRs at 90° or 105°, rather than at 75°, may minimize the risk for graft overload.

The graft forces observed in this study were higher than those in previously reported PCL graft force investigations.[13,14] Harner et al[14] reported calculated in situ forces ranging from 24 to 117 N throughout 0° to 120° of flexion for an applied posterior tibial load of 134 N in an SB PCLR knee with the graft fixed at 90°. In contrast, we report directly measured graft forces ranging from 73 to 155 N throughout 0° to 120° of flexion for a 134-N applied posterior tibial load in an SB PCLR knee similarly fixed at 90°. This disparity may be attributed to differences in force data acquisition methods. In another study, Markolf et al[26] reported decreased graft forces measured at the tibial graft end compared with the femoral end and attributed this finding to frictional losses incurred by the patellar tendon graft as it wrapped around the tibial corner. Additional studies using a femoral force acquisition methodology reported loads in a similar range; however, it is important to distinguish that this methodology prevents the collection of independent graft forces, which was required for part 2 of this study.[24,25] Similar to the study by Harner et al,[14] our study found that graft force increases with knee flexion angle, and both ranged a similar span of graft forces with a range of 82 N (maximal force minus minimal force) for the present study and 93 N for Harner et al. Moreover, this study found that for every 1° increase in flexion angle, there was a 0.67-N increase in graft force. Additionally, both the present study and that by Harner et al reported that the minimum graft force was at 0° of flexion during an applied posterior tibial load and the maximum graft force was at higher flexion angles (90° for Harner et al and 105° for the present study). Despite the difference in graft force values between Harner et al's and our studies, comparable trends were observed for the relationship of graft force versus flexion angle.

We acknowledge limitations to this study. Inherent to a time-zero cadaveric study, the results of this study do not reflect biological healing or graft incorporation effects on reconstruction graft performance. We did not intend to simulate long-term stability that would be observed after thousands of cycles or replicate stability produced by the knee musculature. Also, the application of multiple loading conditions at each flexion angle may have introduced laxity into the surrounding soft tissues structures. This effect was limited by randomizing the order of graft fixation angles and knee flexion angles during testing. The results of this study may apply only to SB PCLRs. Additionally, the measurements of graft forces at the tibial tunnel could result in measurements that do not precisely match the graft forces seen intra-articularly, because of the geometry of the knee and the tibial corner. Previous work[26] using an isometric patellar tendon graft with 2 bone plugs described a loss of force intra-articularly compared with forces at the tibial tunnel; the consistency of this force reduction suggests that increases or decreases in graft force at the tibial tunnel can be used as a surrogate for changes observed intra-articularly due to changes in graft fixation method. Finally, only fixation angles within the most clinically reported range were tested. As seen in Harner et al,[14] investigation of fixation at clinically irrelevant angles, such as full extension, demonstrated rather significant adverse effects, and investigation of such angles may have better emphasized the importance of remaining within the reported range of fixation angles to prevent adverse outcomes.

CONCLUSION

We found that graft fixation angles for SB PCLRs within the clinically reported range of 75° to 105° were successful in significantly improving knee kinematics compared with the sectioned state. However, persistent laxity remained compared with the intact state during posterior tibial loading at all flexion angles, internal rotation at flexion angles ≥60°, and external rotation ≥75° of flexion. SB graft fixation at 75°, 90°, and 105° reduced knee laxity to relatively the same degree, with no significant differences in kinematics among the 3 groups.

ACKNOWLEDGMENT

The authors acknowledge Arthrex Inc for in-kind donations of surgical supplies, Smith & Nephew for an in-kind donation of surgical supplies, AlloSource for the donation of allograft ligament specimens, Kyle Jansson for his graft force fixture design, Brian Devitt, MD, for assistance with study design and surgery, Grant Dornan, MSc, for his assistance in statistical analysis, and Angelica Wedell for photography.

REFERENCES

1. Ahmad CS, Cohen ZA, Levine WN, Gardner TR, Ateshian GA, Mow VC. Codominance of the individual posterior cruciate ligament bundles. An analysis of bundle lengths and orientation. *Am J Sports Med*. 2003;31(2):221-225.
2. Anderson CJ, Ziegler CG, Wijdicks CA, Engebretsen L, LaPrade RF. Arthroscopically pertinent anatomy of the anterolateral and posteromedial bundles of the posterior cruciate ligament. *J Bone Joint Surg Am*. 2012;94(21):1936-1945.
3. Bergfeld JA, Graham SM, Parker RD, Valdevit AD, Kambic HE. A biomechanical comparison of posterior cruciate ligament reconstructions using single- and double-bundle tibial inlay techniques. *Am J Sports Med*. 2005;33(7):976-981.
4. Boutefnouchet T, Bentayeb M, Qadri Q, Ali S. Long-term outcomes following single-bundle transtibial arthroscopic posterior cruciate ligament reconstruction. *Int Orthop*. 2013;37(2):337-343.
5. Cooper DE, Stewart D. Posterior cruciate ligament reconstruction using single-bundle patella tendon graft with tibial inlay fixation: 2- to 10-year follow-up. *Am J Sports Med*. 2004;32(2):346-360.
6. Dennis MG, Fox JA, Alford JW, Hayden JK, Bach BR Jr. Posterior cruciate ligament reconstruction: current trends. *J Knee Surg*. 2004;17(3):133-139.
7. Fanelli GC, Edson CJ. Posterior cruciate ligament injuries in trauma patients: part II. *Arthroscopy*. 1995;11(5):526-529.
8. Galloway MT, Grood ES, Mehalik JN, Levy M, Saddler SC, Noyes FR. Posterior cruciate ligament reconstruction. An in vitro study of femoral and tibial graft placement. *Am J Sports Med*. 1996;24(4):437-445.
9. Gill TJ, Van de Velde SK, Wing DW, Oh LS, Hosseini A, Li G. Tibiofemoral and patellofemoral kinematics after reconstruction of an isolated posterior cruciate ligament injury: in vivo analysis during lunge. *Am J Sports Med*. 2009;37(12):2377-2385.
10. Girgis FG, Marshall JL, Monajem A. The cruciate ligaments of the knee joint. Anatomical, functional and experimental analysis. *Clin Orthop Relat Res*. 1975;106:216-231.
11. Goldsmith MT, Jansson KS, Smith SD, Engebretsen L, LaPrade RF, Wijdicks CA. Biomechanical comparison of anatomic single- and double-bundle anterior cruciate ligament reconstructions: an in vitro study. *Am J Sports Med*. 2013;41(7):1595-1604.
12. Grood ES, Suntay WJ. A joint coordinate system for the clinical description of three-dimensional motions: application to the knee. *J Biomech Eng*. 1983;105(2):136-144.
13. Harner CD, Janaushek MA, Kanamori A, Yagi M, Vogrin TM, Woo SL. Biomechanical analysis of a double-bundle posterior cruciate ligament reconstruction. *Am J Sports Med*. 2000;28(2):144-151.
14. Harner CD, Janaushek MA, Ma CB, Kanamori A, Vogrin TM, Woo SL. The effect of knee flexion angle and application of an anterior tibial load at the time of graft fixation on the biomechanics of a posterior cruciate ligament-reconstructed knee. *Am J Sports Med*. 2000; 28(4):460-465.
15. Harner CD, Xerogeanes JW, Livesay GA, et al. The human posterior cruciate ligament complex: an interdisciplinary study. Ligament morphology and biomechanical evaluation. *Am J Sports Med*. 1995;23(6):736-745.
16. Houe T, Jorgensen U. Arthroscopic posterior cruciate ligament reconstruction: one- vs. two-tunnel technique. *Scand J Med Sci Sports*. 2004;14(2):107-111.
17. Kennedy JC, Grainger RW. The posterior cruciate ligament. *J Trauma*. 1967;7(3):367-377.
18. Kennedy NI, LaPrade RF, Goldsmith MT, et al. Posterior cruciate ligament graft fixation angles, part 2: biomechanical evaluation for anatomic double-bundle reconstruction. *Am J Sports Med*. In press.
19. Kennedy NI, Wijdicks CA, Goldsmith MT, et al. Kinematic analysis of the posterior cruciate ligament, part 1: the individual and collective function of the anterolateral and posteromedial bundles. *Am J Sports Med*. 2013;41(12):2828-2838.
20. Kim YM, Lee CA, Matava MJ. Clinical results of arthroscopic single-bundle transtibial posterior cruciate ligament reconstruction: a systematic review. *Am J Sports Med*. 2011;39(2):425-434.
21. Lien OA, Aas EJ, Johansen S, Ludvigsen TC, Figved W, Engebretsen L. Clinical outcome after reconstruction for isolated posterior cruciate ligament injury. *Knee Surg Sports Traumatol Arthrosc*. 2010; 18(11):1568-1572.
22. Makris CA, Georgoulis AD, Papageorgiou CD, Moebius UG, Soucacos PN. Posterior cruciate ligament architecture: evaluation under microsurgical dissection. *Arthroscopy*. 2000;16(6):627-632.
23. Margheritini F, Rihn JA, Mauro CS, Stabile KJ, Woo SL, Harner CD. Biomechanics of initial tibial fixation in posterior cruciate ligament reconstruction. *Arthroscopy*. 2005;21(10):1164-1171.
24. Markolf KL, Feeley BT, Jackson SR, McAllister DR. Biomechanical studies of double-bundle posterior cruciate ligament reconstructions. *J Bone Joint Surg Am*. 2006;88(8):1788-1794.
25. Markolf KL, Jackson SR, McAllister DR. Single- versus double-bundle posterior cruciate ligament reconstruction: effects of femoral tunnel separation. *Am J Sports Med*. 2010;38(6):1141-1146.
26. Markolf KL, Slauterbeck JR, Armstrong KL, Shapiro MS, Finerman GA. A biomechanical study of replacement of the posterior cruciate ligament with a graft. Part 1: isometry, pre-tension of the graft, and anterior-posterior laxity. *J Bone Joint Surg Am*. 1997;79(3):375-380.
27. Markolf KL, Zemanovic JR, McAllister DR. Cyclic loading of posterior cruciate ligament replacements fixed with tibial tunnel and tibial inlay methods. *J Bone Joint Surg Am*. 2002;84(4):518-524.
28. Mauro CS, Sekiya JK, Stabile KJ, Haemmerle MJ, Harner CD. Double-bundle PCL and posterolateral corner reconstruction components are codominant. *Clin Orthop Relat Res*. 2008;466(9):2247-2254.
29. Papannagari R, DeFrate LE, Nha KW, et al. Function of posterior cruciate ligament bundles during in vivo knee flexion. *Am J Sports Med*. 2007;35(9):1507-1512.
30. Pearsall AT, Pyevich M, Draganich LF, Larkin JJ, Reider B. In vitro study of knee stability after posterior cruciate ligament reconstruction. *Clin Orthop Relat Res*. 1996;327:264-271.
31. Race A, Amis AA. The mechanical properties of the two bundles of the human posterior cruciate ligament. *J Biomech*. 1994;27(1):13-24.
32. Sekiya JK, West RV, Ong BC, Irrgang JJ, Fu FH, Harner CD. Clinical outcomes after isolated arthroscopic single-bundle posterior cruciate ligament reconstruction. *Arthroscopy*. 2005;21(9):1042-1050.
33. Seo YJ, Song SY, Kim IS, Seo MJ, Kim YS, Yoo YS. Graft tension of the posterior cruciate ligament using a finite element model [published online July 14, 2014]. *Knee Surg Sports Traumatol Arthrosc*. doi:10.1007/00167-013-2609-6
34. Spiridonov SI, Slinkard NJ, LaPrade RF. Isolated and combined grade-III posterior cruciate ligament tears treated with double-bundle reconstruction with use of endoscopically placed femoral tunnels and grafts: operative technique and clinical outcomes. *J Bone Joint Surg Am*. 2011;93(19):1773-1780.
35. Van Dommelen BA, Fowler PJ. Anatomy of the posterior cruciate ligament. A review. *Am J Sports Med*. 1989;17(1):24-29.
36. Wang CJ, Chan YS, Weng LH. Posterior cruciate ligament reconstruction using hamstring tendon graft with remnant augmentation. *Arthroscopy*. 2005;21(11):1401.
37. Wang CJ, Chen HS, Huang TW. Outcome of arthroscopic single bundle reconstruction for complete posterior cruciate ligament tear. *Injury*. 2003;34(10):747-751.
38. Wijdicks CA, Kennedy NI, Goldsmith MT, et al. Kinematic analysis of the posterior cruciate ligament, part 2: a comparison of anatomic single- versus double-bundle reconstruction. *Am J Sports Med*. 2013;41(12):2839-2848.
39. Wijdicks CA, Michalski MP, Rasmussen MT, et al. Superficial medial collateral ligament anatomic augmented repair versus anatomic reconstruction: an in vitro biomechanical analysis. *Am J Sports Med*. 2013;41(12):2858-2866.
40. Wu G, Cavanagh PR. ISB recommendations for standardization in the reporting of kinematic data. *J Biomech*. 1995;28(10):1257-1261.